ISPRS Annals of the Photogrammetry, Remote Sensing and Spatial Information Sciences, Volume XII-4/W1-2026
21st International 3D GeoInfo Conference 2026, 28–29 September 2026, Sofia, Bulgaria

Open Urban Simulations All the Way: Extending VoxCity to CityGML and Project PLATEAU

Kunihiko Fujiwara[1], Filip Biljecki[2, 3]

[1] Research & Development Institute, Takenaka Corporation, Japan – fujiwara.kunihiko@takenaka.co.jp
[2] Department of Architecture, National University of Singapore, Singapore - filip@nus.edu.sg
[3] Department of Real Estate, National University of Singapore, Singapore

Keywords: Urban morphology, Voxel, Sunlight exposure, View index, Level of detail, Open geospatial data.

Abstract

CityGML is a prominent standard for semantic 3D city models, and a growing number of open 3D city models are available in this format worldwide. It supports urban simulations, such as assessing microclimate and visual environments, but its potential has not been fully realized due to a lack of free and open-source simulation software compatible with CityGML. Consequently, when data is available in CityGML, it commonly serves its purpose as an exchange format and is converted to other formats. This creates a major bottleneck for the widespread adoption of urban environment simulations since preparing simulation-ready models often entails fixing geometries and resolving conversion issues. To address this shortcoming, we introduce an extension to the open-source Python package "VoxCity" that offers seamless functionality to parse CityGML files, fill in missing data by integrating open geospatial data, generate voxel-based meshes, and perform urban environment simulations. It is one of the few open-source software solutions that are CityGML-compliant. We demonstrate the framework using CityGML data for Tokyo and Osaka from Project PLATEAU—which covers more than 250 cities in Japan—through two use cases: (1) window green views, and (2) pedestrian sunlight exposure. Our package, VoxCity, and the newly developed extension are freely available at https://github.com/kunifujiwara/VoxCity and https://github.com/kunifujiwara/VoxCityGML, respectively. We believe that this framework will facilitate the application of CityGML in urban environment simulations by reducing the time and effort required.

1. Introduction

Urban environment simulation is a powerful tool for informed urban and architectural planning, facilitating the evaluation of thermal stress (Lindberg et al., 2008), pedestrian sunlight exposure (Azegami et al., 2023), building energy consumption (Gros et al., 2016), landmark visibility (Fan et al., 2026), and visual perception (Urech et al., 2022). These simulations require 3D city models with semantic attributes, such as buildings, vegetation, and water bodies, as input data (Taleghani et al., 2016). The intensive manual effort required to prepare these input models has hindered the widespread application of urban environment simulations.

Concurrently, an increasing number of semantic 3D city models are being developed for cities worldwide (Lei et al., 2023). One widely used file format is CityGML, a standardized data structure for 3D city models that enables the storage and exchange of urban 3D geometry and semantics (Kolbe et al., 2005; Kolbe, 2009; Gröger and Plümer, 2012). Open 3D city models in the CityGML format have significant potential to scale the application of urban environment simulations by offering readily available input data (Kutzner et al., 2020; Lei and Biljecki, 2025). However, the CityGML format is not directly compatible with most existing simulation packages. Users must convert it to other formats and repair its geometry to meet the quality requirements of specific simulation software. Consequently, the advent of open 3D city models in the CityGML format has not yet significantly facilitated the adoption of environment simulations in urban studies and practical urban and architectural planning projects.

In this paper, we present an open-source simulation framework that directly leverages 3D city models in the CityGML format. We demonstrate two specific use cases that evaluate (1) window green views, and (2) pedestrian solar irradiance. As an extension of Use Case 2, we apply our approach to multiple building LoDs and investigate the impact of LoD on simulated pedestrian solar irradiance.

2. Framework

Our framework adopts the existing Python package "VoxCity" (Fujiwara et al., 2026), which offers seamless functionality for open geospatial data integration, 3D city model generation, and urban environment simulation. VoxCity originally did not support CityGML as an input format; therefore, we developed an extension enabling the package to leverage 3D city models in this format for model generation and simulation. This study specifically focuses on Project PLATEAU[1], which has released open 3D city models in the CityGML format for over 250 cities in Japan, but the approach can be generalized elsewhere.

This work is one of only a few open-source frameworks, including 3DCityDB (Yao et al., 2018) and City4CFD (Pađen et al., 2024), that directly accept the CityGML format for urban environment simulation. While 3DCityDB efficiently manages spatial databases and City4CFD processes geometries specifically for Computational Fluid Dynamics (CFD) simulations, these existing tools rely on external software packages to perform the actual urban environment simulations. Consequently, our framework offers more seamless and comprehensive functionality in urban environment simulations. The following subsections provide an overview of the original VoxCity package and detail its newly developed CityGML extension.

2.1 The VoxCity package

Fujiwara et al. (2026) already detailed VoxCity's original func-

[1] https://www.mlit.go.jp/plateau/

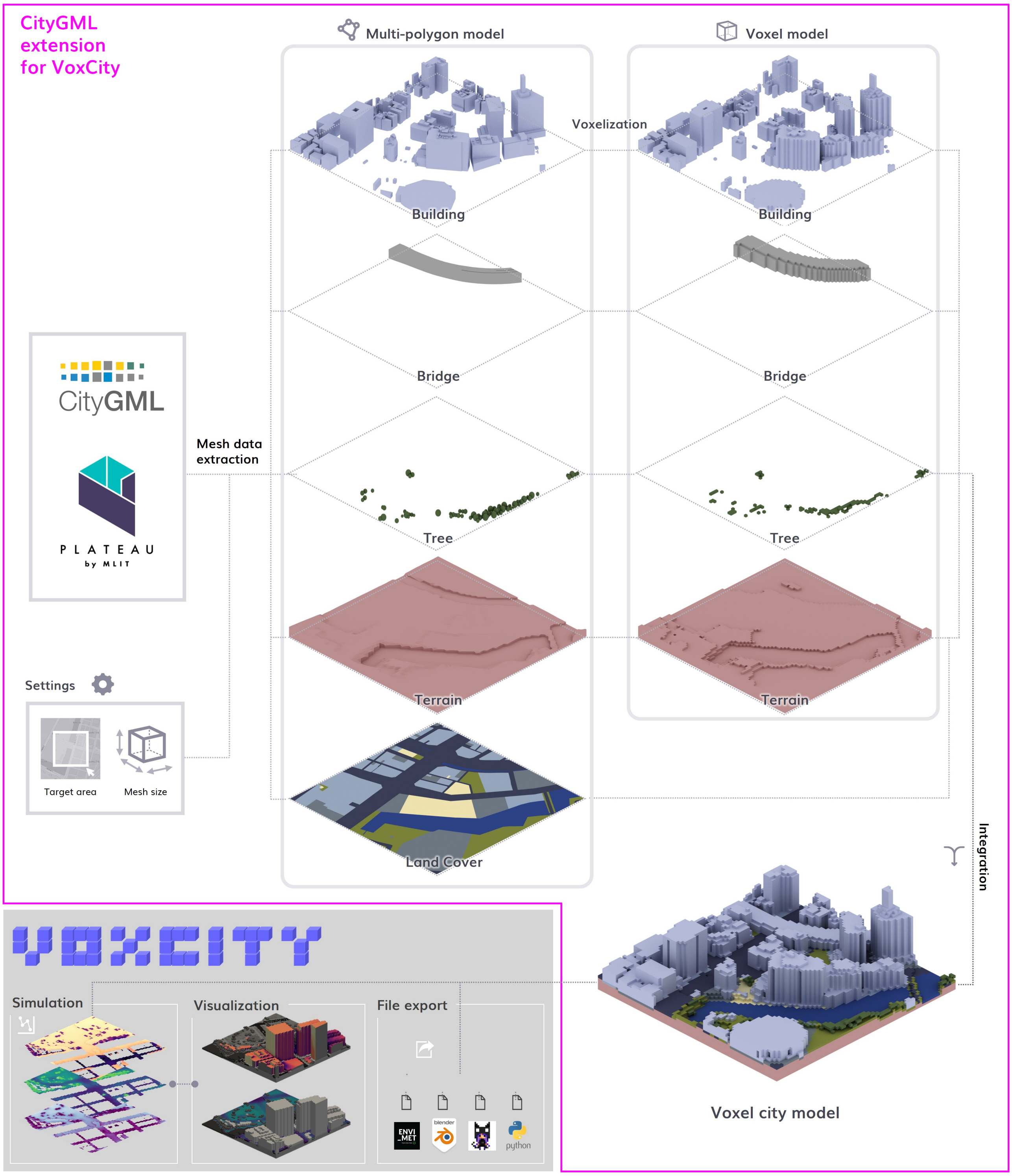

Figure 1. Framework of our CityGML extension for VoxCity, adapted to suit Project PLATEAU.

tionality; therefore, this subsection presents a brief overview of its features.

Download: VoxCity downloads building footprints and heights, tree canopy heights, land cover, and terrain elevation data within a specified target area from open data sources. The data sources incorporated in VoxCity include, for instance, OpenStreetMap[2] (OSM) for buildings, OpenEarthMap Japan (Yokoya et al., 2024) for land cover, Global Canopy Height Maps (Tolan et al., 2024) for tree canopy height, and FABDEM (Hawker et al., 2022) for terrain elevation. **Voxelization and integration:** Using the downloaded data, VoxCity creates voxel models for buildings, trees, land cover, and terrain, and integrates them to generate voxel city models with semantic attributes. This step also serves as a meshing process for subsequent simulations. **Simulation:** VoxCity features a built-in "simulator" subpackage for urban environment simulations. The subpackage provides capabilities for simulating solar irradiance at street level and on building surfaces, calculating view

[2] `https://www.openstreetmap.org`

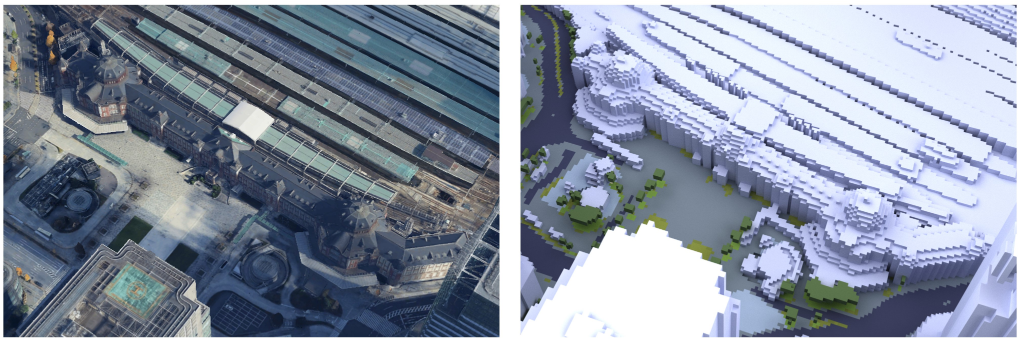

Figure 2. An example voxel city model compared with the actual urban morphology derived from Google Photorealistic 3D Tiles.

indices such as the Green View Index (GVI) (Li et al., 2015) and Sky View Index (SVI) (Yang et al., 2024), and assessing landmark visibility. **Visualization:** VoxCity offers built-in visualization functions that enable both 2D and 3D visualization of simulation results. Users can visualize 3D simulation results on building surfaces (e.g., solar irradiance and sky view factor) and at street level (e.g., landmark visibility) without requiring external rendering software. **File export:** VoxCity can export the generated 3D city models in several file formats compatible with external software such as ENVI-met[3] for microclimate simulation, Blender[4] and Rhino[5] for 3D modeling and rendering, and MagicaVoxel[6] for voxel-dedicated modeling and rendering.

2.2 CityGML extension for VoxCity

This extension extracts the required information from the CityGML format to create voxel city models (Figure 1). The original VoxCity primarily handles LoD1 buildings represented by footprints and height values, whereas this extension is compatible with LoD2+ buildings; therefore, it can handle complex 3D shapes and simulate the urban environment more precisely. Figure 2 shows an example voxel city model compared with the actual urban morphology.

More specifically, the extension extracts information on buildings, bridges, trees, land cover, and terrain from the CityGML format (Figure 1). CityGML defines Building, Bridge, Tunnel, CityFurniture, CityObjectGroup, LandUse, Relief, Transportation, Vegetation, and WaterBody as city objects in its data structure (Kolbe et al., 2005). Among these, our extension incorporates Building, Bridge, Vegetation, LandUse, and Relief (terrain). For Building, Bridge, and Vegetation objects in LoD2+, the extension creates watertight solid meshes based on 3D multipolygon data in CityGML and voxelizes them. For Relief, the extension creates watertight solids by extruding triangular terrain meshes and then voxelizes them. Additionally, it converts LandUse to land cover data using conversion rules and projects the land cover classes onto the topmost voxels of the terrain.

Our approach can combine the information extracted from CityGML with open geospatial data that can be downloaded using the original functionality of VoxCity. For example, PLATEAU provides vegetation data for only a few limited areas; however, VoxCity can compensate for this lack of tree information using open datasets, such as Global Canopy Height Maps (Tolan et al., 2024) and OpenEarthMap Japan (Yokoya et al., 2024). A key advantage of our approach is this ability to combine data, allowing users to complement missing information in CityGML models.

[3] `https://envi-met.com/`
[4] `https://www.blender.org/`
[5] `https://www.rhino3d.com/`
[6] `https://ephtracy.github.io/index.html?page=mv_main`

3. Use cases

As mentioned in Section 1, there are diverse utilities of urban environment simulations. Among them, we focus on green visibility and solar irradiance to demonstrate use cases of our framework. Numerous studies have investigated urban green views and reported their impact on perceived comfort and mental health (Cheng et al., 2026; Elsadek et al., 2020; Lei et al., 2026). Many of them rely on street view imagery and computer vision techniques and evaluate visibility from pedestrian perspectives, owing to emerging global data sources such as Google Street View and Mapillary. Meanwhile, window green views have been less investigated due to a lack of available imagery data sources from window perspectives or 3D city models with vegetation objects.

Regarding solar irradiance, an increasing number of studies have examined pedestrian sunlight exposure for its importance in assessing heat stress, skin health, and walkability (Azegami et al., 2023; Li et al., 2023; Fujiwara et al., 2024). Frequent heat waves caused by climate change and the urban heat island effect have also contributed to this growing attention. Additionally, numerous datasets for LoD1 building data have been released owing to recent advancements in computer vision techniques and a growing number of data providers for satellite or aerial imagery (Zhu et al., 2025; Microsoft, 2024). It is therefore important to explore the usability of this simplified building geometry in evaluating pedestrian sunlight exposure.

3.1 Window green view

As an indicator to evaluate window green views, we define the Window Green View Index (WGVI), which quantifies the visibility of plant objects, including trees and vegetated land cover, from the meshes of vertical building surfaces. We calculated the WGVI for two target areas in Tokyo and Osaka using the CityGML extension for VoxCity and VoxCity's built-in simulation module for visibility calculation. Both target areas cover a 2 km by 2 km extent and are centered at Tokyo Station and Osaka Station. We used LoD2 buildings and terrain elevation from PLATEAU, while employing land cover and tree positions from OpenEarthMap Japan. The voxel size used was 2 m. To accurately calculate the WGVI for buildings at the perimeter (near the boundary edges), we generated voxel city models not

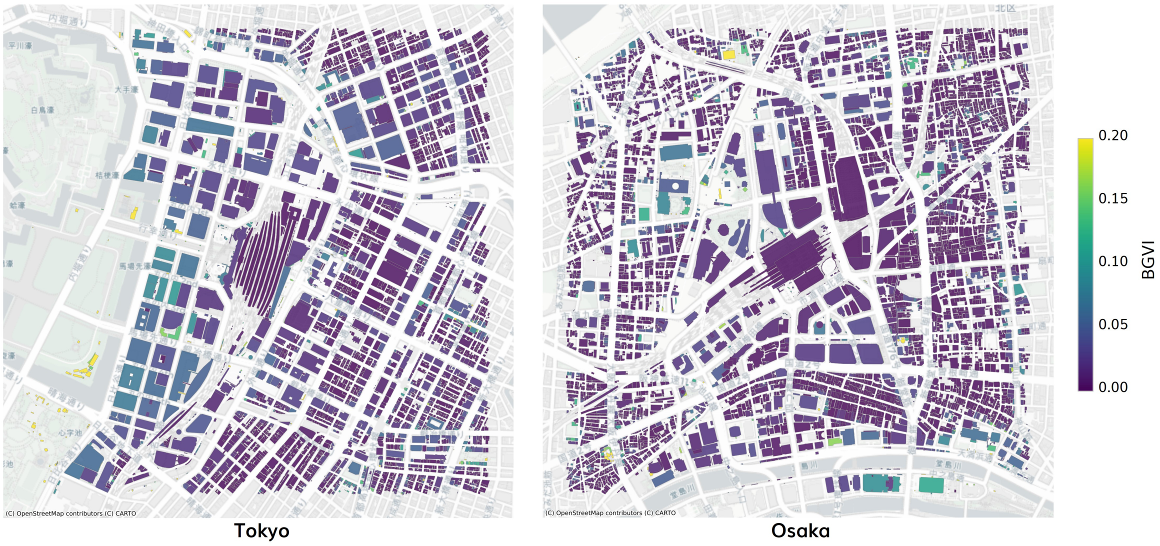

Figure 3. Maps of the average Window Green View Index of individual buildings.

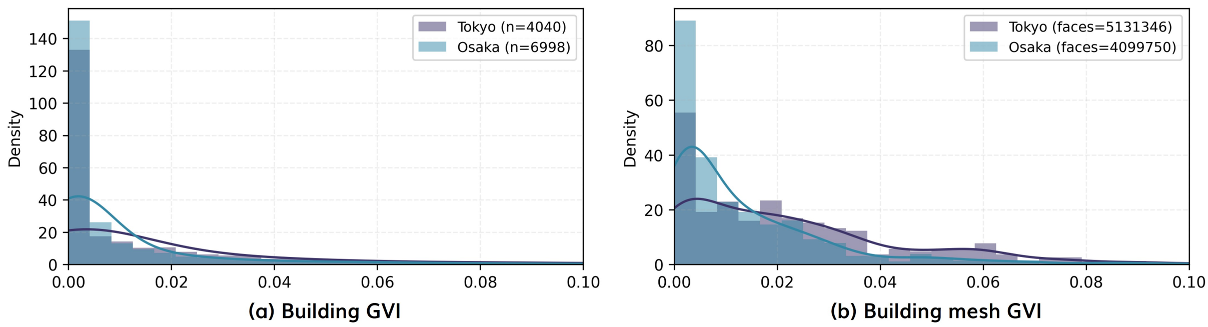

Figure 4. Histograms of per-building and per-mesh Window Green View Index.

only for the target areas but also for an outside buffer with a 1 km width. Consequently, WGVI calculations were conducted using areas of 4 km by 4 km.

Figure 3 shows the spatial distribution of the per-building mean WGVI. The majority of buildings in both areas exhibit low WGVI values, reflecting the dense, vegetation-poor character of those urban cores. Isolated buildings with moderate to high WGVI values are scattered throughout both areas, corresponding to their proximity to street trees and vegetated parks. Tokyo displays a relatively broad spatial distribution of moderately green buildings across its grid, especially in areas near the Imperial Palace, which is located to the west.

Figure 4 illustrates the frequency distributions of the WGVI at two scales of analysis: (a) per-building and (b) per-mesh. For per-building WGVI, both cities exhibit a strongly right-skewed distribution, with the majority of buildings concentrated near zero, underscoring the rarity of window views with rich green presence in dense urban environments. For per-mesh WGVI, Tokyo's distribution becomes noticeably flatter and more spread out relative to Osaka's, indicating greater heterogeneity in green visibility across building surfaces.

We believe that such window view simulations can be applied to city-scale analyses for evaluating the impact of scenery from windows on residents' mental health or real estate prices, consequently supporting informed planning decisions for sustainable urban development.

3.2 Pedestrian sunlight exposure

We conducted street-level (1.5 m from the ground) simulations of cumulative solar irradiance for August using the same target areas and 3D city model as in Section 3.1, alongside VoxCity's built-in simulation functions. We calculated Cumulative Global Horizontal Solar Irradiance (CGHI) using hourly input solar irradiance data from EnergyPlus Weather (EPW) files and solar position data calculated by the Python package 'astral'[7]. We employed the nearest EPW files from Climate.OneBuilding.Org[8] for each area. The accumulation period was the entire month of August (from August 1 to August 31). Further details of the solar irradiance simulation can be found in the VoxCity paper by Fujiwara et al. (2026). Additionally, we aggregated CGHI along road networks downloaded from OSM using OSMnx (Boeing, 2017) with the road tag "walk".

Figure 5 shows the calculated CGHI for the target areas in Tokyo and Osaka. Overall, Tokyo shows relatively low CGHI compared to Osaka, indicating shading by Tokyo's denser building morphology. Figure 6 shows the histogram of the per-network-edge mean CGHI. Tokyo has its mode at a significantly lower value compared to Osaka, confirming the lower CGHI and denser building shading in Tokyo. It is important to note that differences in the input solar irradiance from EPW data

[7] `https://github.com/sffjunkie/astral`
[8] `https://climate.onebuilding.org`

https://doi.org/10.5194/isprs-annals-XII-4-W1-2026-137-2026

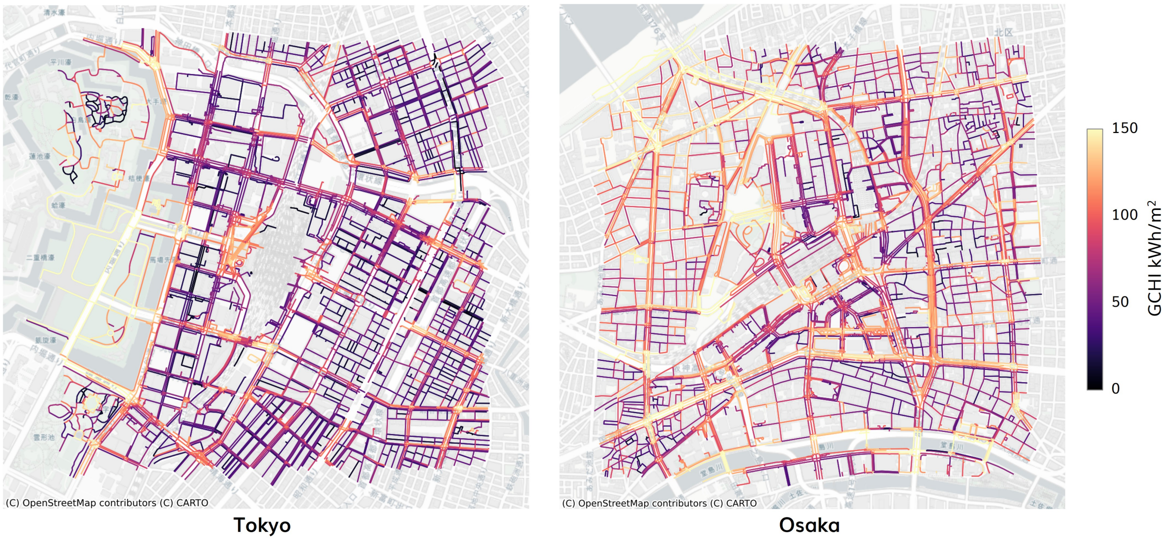

Figure 5. Maps of Cumulative Global Horizontal Solar Irradiance aggregated on walking path networks.

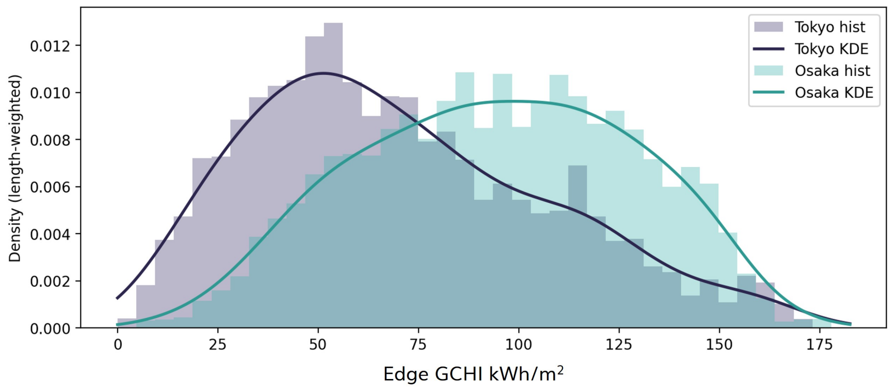

Figure 6. Histogram of edge CGHI.

may have affected this heterogeneity. The higher sunlight exposure in Osaka suggests a significant need for additional shading, such as planting trees or installing artificial structures. We believe that such sunlight exposure analyses can help inform urban design to create well-shaded and walkable streets.

3.3 Impact of building LoD on simulated pedestrian sunlight exposure

Many building height datasets employ LoD1, which cannot represent complex building shapes featuring, for example, pilotis or setbacks in building walls. For applications of 3D city models in urban environment simulations, such as pedestrian sunlight exposure analysis, the simplification of LoD1 could cause significant calculation errors. Therefore, we conducted a comparative analysis to evaluate the impact of building LoD on pedestrian sunlight exposure as a use case of our approach. This use case also doubles as a demonstration of the multi-LoD capabilities of the developed approach. Specifically, we calculated CGHI aggregated along road networks for both the LoD1 building case and the LoD2 building case, and then compared the CGHI of the two cases. We used the same simulation settings as those used for the Tokyo case in Section 3.2.

Figure 7 shows the difference in CGHI between the LoD1 and LoD2 cases, accompanied by images of voxel city models comparing the two cases. For most edges, the CGHI difference ranges from -12 to +12 kWh/m^2 and exhibits a heterogeneous geospatial distribution. That is, LoD1 simplification causes underestimation in some areas and overestimation in others. Voxel city models of the area with significant overestimation show that a high-rise building exhibits significantly lower building height in LoD1 than that in LoD2. We attributed the overestimation of pedestrian sunlight exposure to this underestimation of building height. Meanwhile, models of the area with underestimation indicate that LoD1 buildings have building top heights identical to those of LoD2. When a building has walls with setbacks, an LoD1 building representation with the same top height as an LoD2 building can cause a substantial overestimation of building volume and its shading effects, and consequently, an underestimation of pedestrian sunlight exposure.

Figure 8 shows a KDE scatter plot of CGHI values derived from LoD1 vs those from LoD2, accompanied by statistical error metrics including RMSE, MAE, and R^2. The KDE scatter plot shows that most network edges have identical CGHI values regardless of the building LoD. RMSE and MAE were 5.7 kWh/m^2 and 3.2 kWh/m^2, respectively, indicating that the error introduced by LoD1 simplification was relatively small compared to the maximum CGHI values of around 150 kWh/m^2. An R^2 of 0.97 also indicates insignificant error caused by LoD1. Although Figures 7 and 8 show some overestimation and underestimation caused by LoD1 simplification, the errors in the

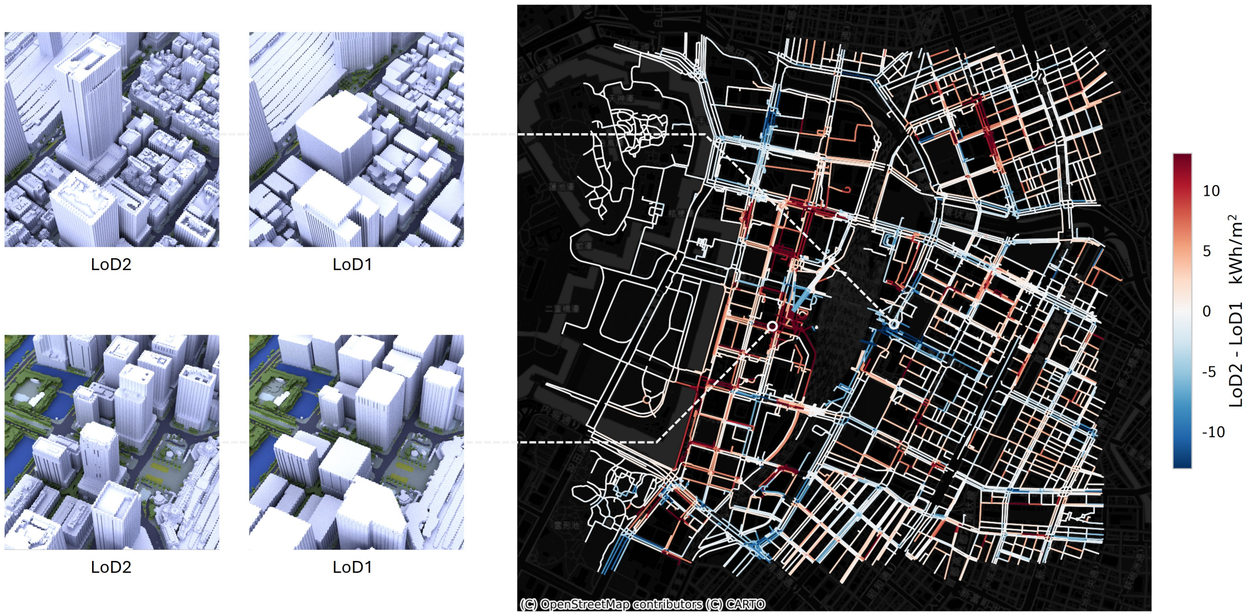

Figure 7. Maps of difference in edge CGHI.

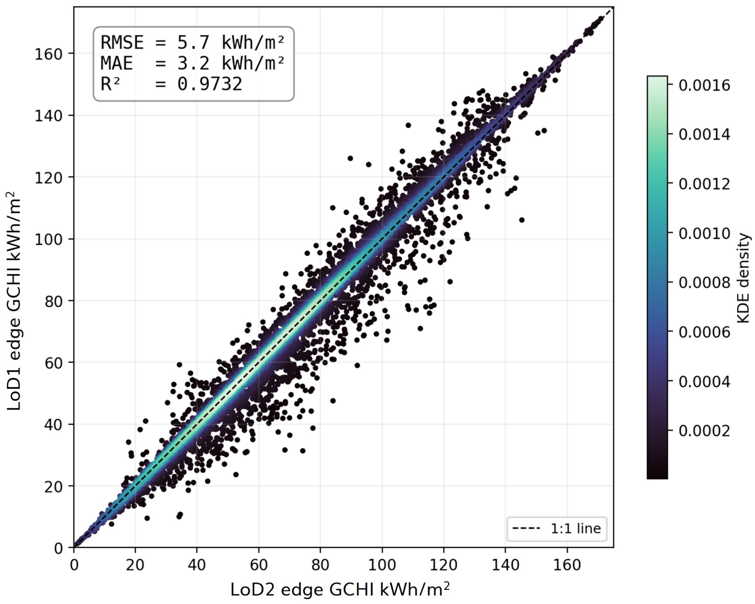

Figure 8. KDE scatter plot of CGHI values derived from LoD1 vs those from LoD2.

target area were not substantial overall.

As showcased in this section, we believe that our approach will facilitate analyses to evaluate the impact of LoD on the simulated urban environment, including not only sunlight exposure but also thermal comfort, wind speed, and the visual environment.

3.4 Manual and computational processing time

Table 1 shows the manual and computational processing times of each use case. All computations were performed on a desktop workstation equipped with an Intel Core i9-13900KF processor (18 cores, 26 logical processors, 3.0 GHz base clock), 64 GB DDR5 RAM (4800 MHz), and an NVIDIA GeForce RTX 4090 GPU (24 GB GDDR6X VRAM). The manual processing time was 9 min for both Use Case 1 (window green views) and Use Case 2 (pedestrian sunlight exposure). This highlights VoxCity's capability to enhance reproducibility of such urban environment simulations, which in turn facilitates comparative analysis among multiple cities. It is important to note that the manual processing time could vary to some extent depending on the user's operation skills. The computational processing took a significantly longer time than the manual processing, 33 and 16 min respectively; however, we believe this will not be a critical barrier because users can work on other tasks during the processing time.

4. Limitations and future directions

While we have demonstrated the capabilities of our framework, we have not yet confirmed that our extension for VoxCity can be applied to CityGML data beyond that provided by Pro-

Table 1. Manual and computational processing time for each use case. Use Case 1 and Use Case 2 represent the processing to create Tokyo in Figure 3 and Figure 5, respectively.

Case	Processing type	Total	Breakdown
Use Case 1	Manual	9 min	• Downloading CityGML data: 6 min • Specifying target area: 1 min • Setting other parameters (mesh size, buffer width, etc.): 2 min
	Computational	33 min	• Parsing CityGML data and generating a voxel city model: 15 min • Calculating Green View Index on building surfaces: 18 min
Use Case 2	Manual	9 min	Same as Use Case 1
	Computational	16 min	• Parsing CityGML data and generating a voxel city model: 15 min • Calculating ground-level cumulative solar irradiance: 1 min

ject PLATEAU. Although all CityGML files adhere to standardized formatting rules, implementation details may vary depending on project objectives and regional specifications. For example, geometric variation such as non-watertight or self-intersecting solids and inconsistent LoD representation across features, as well as attribute-level differences such as provider-specific LandUse classifications, may require additional handling not yet implemented in our current extension. Therefore, it is essential to refine our methods to ensure generalizability across diverse CityGML datasets from various urban environments.

VoxCity currently does not incorporate several CityGML object types, including Tunnel, CityFurniture, CityObjectGroup, Transportation, and WaterBody. The integration of these native CityGML object types would enhance the accuracy and comprehensiveness of our semantic 3D city model generation and urban environment simulations. Future work may also incorporate higher LoD models such as LoD3. While they are scarce, recent methods have been developed to extract window information at scale (Ma et al., 2026), which could benefit the use case of window green views.

Additionally, CityJSON provides a developer-friendly, compact, and web-ready alternative to CityGML by replacing complex XML hierarchies with a flattened JSON structure and efficient vertex indexing, drastically reducing file size and parsing effort (Ledoux et al., 2019). We plan to extend our framework to this format as well.

Furthermore, while VoxCity adopts established methods for solar and visibility simulation, the results have not yet been validated against measured data or existing benchmark software. It is desirable to conduct measurements for solar irradiance and view indices using pyranometers and panoramic cameras, and to perform benchmark comparisons using existing voxel-based simulation models such as PALM (Maronga et al., 2020) and ENVI-met[9]. Voxel mesh size is likely to significantly affect simulation accuracy; therefore, in addition to validating the simulation models, a quantitative assessment of its impact on accuracy is needed.

Addressing these structural limitations will be a crucial step toward establishing urban digital twins with simulated environmental metrics (Ignatius et al., 2024), while requiring minimal manual effort. Furthermore, coupling our static framework with dynamic data will enable continuous monitoring of urban microclimate and human-centric designs.

[9] `https://envi-met.com/`

5. Conclusion

An increasing number of semantic 3D city models have been released in the CityGML format by cities worldwide (Lei et al., 2023); however, the adoption of this format in urban environment simulations has been limited, primarily due to a lack of compatible software packages. To address this issue, we introduced an extension of an open-source framework for urban environment simulations that offers native support for CityGML. Specifically, we developed a CityGML extension for VoxCity, a Python package that offers seamless functionality for open geospatial data integration, voxel-based 3D city model generation, and urban environment simulation. By applying this framework to analyze window green views, pedestrian sunlight exposure, and the impact of building LoD on solar irradiance, we demonstrated its practical utility for urban environment analyses. The main contributions of this work are as follows:

1. Our framework provides a seamless, streamlined, and automatic method from downloading a CityGML file, through voxel-based meshing and urban environment simulation, to visualization of 3D simulation results. This significantly reduces the time and effort required and enables city-scale simulations with only around 10 minutes of manual processing time. This enhances the reproducibility of urban environment simulations, and in turn, facilitates comparative analysis across cities.

2. Our CityGML extension for VoxCity can supplement missing information in CityGML files with open geospatial data, including tree canopy height, land cover, and water bodies, to create an integrated semantic voxel city model for urban environment simulations.

3. Our method is released as an open-source Python package, enabling users to easily modify and incorporate it into their own frameworks.

References

Azegami, Y., Imanishi, M., Fujiwara, K., Kusaka, H., 2023. Effects of solar radiation in the streets on pedestrian route choice in a city during the summer season. *Build. Environ.*, 235, 110250.

Boeing, G., 2017. OSMnx: New methods for acquiring, constructing, analyzing, and visualizing complex street networks. *Comput. Environ. Urban Syst.*, 65, 126–139.

Cheng, S., Lei, B., Fujiwara, K., Miller, C., Biljecki, F., van Ameijde, J., 2026. Walking through green and grey: Exploring sequential exposure and multisensory environmental effects on psychological restoration. *Build. Environ.*, 287(113748), 113748.

Elsadek, M., Liu, B., Xie, J., 2020. Window view and relaxation: Viewing green space from a high-rise estate improves urban dwellers' wellbeing. *Urban For. Urban Green.*, 55(126846), 126846.

Fan, Z., Fujiwara, K., Liu, P., Zhang, F., Biljecki, F., 2026. From street view to visibility network: Mapping urban visual relationships with vision-language models. *arXiv [cs.CV]*.

Fujiwara, K., Ito, K., Ignatius, M., Biljecki, F., 2024. A panorama-based technique to estimate sky view factor and solar irradiance considering transmittance of tree canopies. *Build. Environ.*, 266(112071), 112071.

Fujiwara, K., Tsurumi, R., Kiyono, T., Fan, Z., Liang, X., Lei, B., Yap, W., Ito, K., Biljecki, F., 2026. VoxCity: A seamless framework for open geospatial data integration, grid-based semantic 3D city model generation, and urban environment simulation. *Comput. Environ. Urban Syst.*, 123(102366), 102366.

Gros, A., Bozonnet, E., Inard, C., Musy, M., 2016. Simulation tools to assess microclimate and building energy – A case study on the design of a new district. *Energy Build.*, 114, 112–122.

Gröger, G., Plümer, L., 2012. CityGML – Interoperable semantic 3D city models. *ISPRS J. Photogramm. Remote Sens.*, 71, 12–33.

Hawker, L., Uhe, P., Paulo, L., Sosa, J., Savage, J., Sampson, C., Neal, J., 2022. A 30m global map of elevation with forests and buildings removed. *Environ. Res. Lett.*, 17(2), 024016.

Ignatius, M., Lim, J., Gottkehaskamp, B., Fujiwara, K., Miller, C., Biljecki, F., 2024. Digital twin and wearables unveiling pedestrian comfort dynamics and walkability in cities. *ISPRS Ann. Photogramm. Remote Sens. Spat. Inf. Sci.*, 10, 195–202.

Kolbe, T. H., 2009. Representing and exchanging 3D city models with CityGML. *Lecture Notes in Geoinformation and Cartography*, Lecture notes in geoinformation and cartography, Springer Berlin Heidelberg, Berlin, Heidelberg, 15–31.

Kolbe, T. H., Gröger, G., Plümer, L., 2005. CityGML: Interoperable access to 3D city models. *Geo-information for Disaster Management*, Springer Berlin Heidelberg, Berlin, Heidelberg, 883–899.

Kutzner, T., Chaturvedi, K., Kolbe, T. H., 2020. CityGML 3.0: New Functions Open Up New Applications. *PFG – Journal of Photogrammetry, Remote Sensing and Geoinformation Science*, 88(1), 43–61. http://dx.doi.org/10.1007/s41064-020-00095-z.

Ledoux, H., Arroyo Ohori, K., Kumar, K., Dukai, B., Labetski, A., Vitalis, S., 2019. CityJSON: a compact and easy-to-use encoding of the CityGML data model. *Open Geospat. Data Softw. Stand.*, 4(1), 4.

Lei, B., Biljecki, F., 2025. Evaluating the development of open 3D city models: a multidimensional assessment. *ISPRS Annals of the Photogrammetry, Remote Sensing and Spatial Information Sciences*, X-4/W6-2025, 137–144.

Lei, B., Liu, P., Fujiwara, K., Frei, M., Miller, C., Chua, Y. X., Biljecki, F., 2026. Multidimensional analysis of human outdoor comfort: Integrating just-in-time adaptive interventions (JITAIs) in urban digital twins. *Cities*, 168(106443), 106443.

Lei, B., Stouffs, R., Biljecki, F., 2023. Assessing and benchmarking 3D city models. *Int. J. Geogr. Inf. Sci.*, 37(4), 788–809.

Li, X., Zhang, C., Li, W., Ricard, R., Meng, Q., Zhang, W., 2015. Assessing street-level urban greenery using Google Street View and a modified green view index. *Urban For. Urban Greening*, 14(3), 675–685.

Li, Y., Huang, N., He, J., 2023. Analytical evaluation of thermal comfort in the pedestrian environment using pedestrian shade space distribution. *Urban Clim.*, 51(101665), 101665.

Lindberg, F., Holmer, B., Thorsson, S., 2008. SOLWEIG 1.0–modelling spatial variations of 3D radiant fluxes and mean radiant temperature in complex urban settings. *Int. J. Biometeorol.*, 52(7), 697–713.

Ma, R., Yang, C., Chen, J., Biljecki, F., Li, X., 2026. Street view imagery-based method for reconstructing 3D building façade openings. *Automation in Construction*, 184, 106842.

Maronga, B., Banzhaf, S., Burmeister, C., Esch, T., Forkel, R., Fröhlich, D., Fuka, V., Gehrke, K. F., Geletič, J., Giersch, S., Gronemeier, T., Groß, G., Heldens, W., Hellsten, A., Hoffmann, F., Inagaki, A., Kadasch, E., Kanani-Sühring, F., Ketelsen, K., Khan, B. A., Knigge, C., Knoop, H., Krč, P., Kurppa, M., Maamari, H., Matzarakis, A., Mauder, M., Pallasch, M., Pavlik, D., Pfafferott, J., Resler, J., Rissmann, S., Russo, E., Salim, M., Schrempf, M., Schwenkel, J., Seckmeyer, G., Schubert, S., Sühring, M., von Tils, R., Vollmer, L., Ward, S., Witha, B., Wurps, H., Zeidler, J., Raasch, S., 2020. Overview of the PALM model system 6.0. *Geosci. Model Dev.*, 13(3), 1335–1372.

Microsoft, 2024. Microsoft building footprints. Accessed: 2024-11-14.

Pađen, I., Peters, R., García-Sánchez, C., Ledoux, H., 2024. Automatic high-detailed building reconstruction workflow for urban microscale simulations. *Build. Environ.*, 265(111978), 111978.

Taleghani, M., Sailor, D., Ban-Weiss, G. A., 2016. Micrometeorological simulations to predict the impacts of heat mitigation strategies on pedestrian thermal comfort in a Los Angeles neighborhood. *Environ. Res. Lett.*, 11(2), 024003.

Tolan, J., Yang, H.-I., Nosarzewski, B., Couairon, G., Vo, H. V., Brandt, J., Spore, J., Majumdar, S., Haziza, D., Vamaraju, J., Moutakanni, T., Bojanowski, P., Johns, T., White, B., Tiecke, T., Couprie, C., 2024. Very high resolution canopy height maps from RGB imagery using self-supervised vision transformer and convolutional decoder trained on aerial lidar. *Remote Sens. Environ.*, 300(113888), 113888.

Urech, P. R. W., Mughal, M. O., Bartesaghi-Koc, C., 2022. A simulation-based design framework to iteratively analyze and shape urban landscapes using point cloud modeling. *Comput. Environ. Urban Syst.*, 91(101731), 101731.

Yang, W., Li, Y., Liu, Y., Fan, P., Yue, W., 2024. Environmental factors for outdoor jogging in Beijing: Insights from using explainable spatial machine learning and massive trajectory data. *Landsc. Urban Plan.*, 243(104969), 104969.

Yao, Z., Nagel, C., Kunde, F., Hudra, G., Willkomm, P., Donaubauer, A., Adolphi, T., Kolbe, T. H., 2018. 3DCityDB - a 3D geodatabase solution for the management, analysis, and visualization of semantic 3D city models based on CityGML. *Open Geospat. Data Softw. Stand.*, 3(1).

Yokoya, N., Xia, J., Broni-Bediako, C., 2024. Submeter-level land cover mapping of Japan. *Int. J. Appl. Earth Obs. Geoinf.*, 127, 103660.

Zhu, X. X., Chen, S., Zhang, F., Shi, Y., Wang, Y., 2025. GlobalBuildingAtlas: an open global and complete dataset of building polygons, heights and LoD1 3D models. *Earth Syst. Sci. Data*, 17(12), 6647–6668.